

1 **Ambient measurement of fluorescent aerosol particles with a WIBS in the Yangtze**
2 **River Delta of China: potential impacts of combustion-related aerosol particles**

3 X. Yu^{1,2}, Z. Wang², M. Zhang², U. Kuhn², Z. Xie¹, Y. Cheng², U. Pöschl², H. Su²

4 ¹School of Earth and Space Sciences, University of Science and Technology of China,
5 Hefei 230026, China

6 ²Multiphase Chemistry Department, Max Planck Institute for Chemistry, Mainz 55128,
7 Germany

8

9 Correspondence to Zhibin Wang (Zhibin.Wang@mpic.de) and Zhouqing Xie
10 (zqxie@ustc.edu.cn)

11

12 **Abstract**

13 Fluorescence characteristics of aerosol particles in polluted atmosphere were studied
14 using a wideband integrated bioaerosol spectrometer (WIBS-4A) in Nanjing, Yangtze
15 River Delta area of China. We observed strong diurnal and day-to-day variations of
16 fluorescent aerosol particles (FAPs). The average number concentrations of FAPs (1-15
17 μm) detected in the three WIBS measurement channels (FL1: 0.6 cm^{-3} , FL2: 3.4 cm^{-3} ,
18 FL3: 2.1 cm^{-3}) were much higher than those observed in forests and rural areas,
19 suggesting that FAPs other than bioaerosols were detected. We found that the number
20 fractions of FAPs were positively correlated with the black carbon mass fraction,
21 especially for the FL1 channel, indicating a large contribution of combustion-related
22 aerosols. To distinguish bioaerosols from combustion-related FAPs, we investigated two
23 classification schemes for use with WIBS data. Our analysis suggests a strong size
24 dependence for the fractional contributions of different types of FAPs. In the FL3 channel,
25 combustion-related particles seem to dominate the 1-2 μm size range while bioaerosols
26 dominate 2-5 μm . The number fractions of combustion-related particles and non-
27 combustion-related particles to total aerosol particles were $\sim 11\%$ and $\sim 5\%$, respectively.

28

29

30 **1 Introduction**

31 From the beginning of atmospheric aerosols studies, airborne biological particles
32 have been found as an important class of aerosol particles (Bary et al., 1887; Haldane and
33 Anderson, 1887; Despr es et al., 2012). They are ubiquitous in the atmosphere with a wide
34 size range from approximately several nanometers to a few hundred micrometers (P oschl,
35 2005; Despr es et al., 2012). Primary biological aerosol particles (PBAPs) are a subset of
36 biological particles, usually defined as the aerosols of biological origin or carry living
37 organisms, including viruses, bacteria, fungal, pollen, cell or plant debris and animal
38 tissue (Huffman et al., 2012). PBAPs can affect the Earth's radiation balance directly by
39 absorbing and scattering solar radiation, and indirectly by serving as giant cloud
40 condensation nuclei (CCN) and ice nuclei (IN), and thereby influence cloud
41 microphysical and climate-relevant properties (Christner et al., 2008; P oschl et al., 2010;
42 Deleon-Rodriguez et al., 2013; Morris et al., 2013). These impacts are not only restricted
43 to a local scale, but may also be effective in a regional scale due to the transport of
44 bioaerosols, e.g., by dust storms (Griffin, 2007; Polymenakou et al., 2008; Hallar et al.,
45 2011; Creamean et al., 2013). In addition, PBAPs can spread human, animal and plant
46 disease and influence public health (Despr es et al., 2012; Cao et al., 2014). Considering
47 its comprehensive impacts in diverse scientific fields, a better understanding of PBAPs
48 such as its concentration, composition, spatial and temporal variability becomes critically
49 important.

50 Despite its importance, information of PBAPs in the atmosphere is still very limited.
51 Further investigation is hindered due to the lack of automatic measurement techniques.
52 Most previous studies are based on the analysis of cultivable PBAPs or DNAs from filter
53 samples (Henningson and Ahlberg, 1994; Duchaine et al., 2001; Yu et al., 2013). [These](#)
54 [methods are time-consuming and their results may differ depending on the cultivation](#)
55 [condition and procedures, especially considering the ubiquity of microorganisms that](#)
56 [cannot be cultivated \(Oliver, 2005; P ohlker et al., 2012\)](#). The low time resolution of
57 cultivation methods makes it difficult to investigate the emission mechanisms of PBAPs,
58 which happen at a time scale of less than a few hours.

59 Since most biological materials contain fluorophores, instruments based on the
60 fluorescence detection, such as UV-APS (Ultraviolet Aerodynamic Particle Sizer)
61 (Brosseau et al., 2000), WIBS (Wideband Integrated Bioaerosol Spectrometer) and other
62 custom-made instruments based on the LIF (Laser induced fluorescence) technology (Pan
63 et al., 2009; Taketani et al., 2013; Miyakawa et al., 2015), have recently been developed
64 for online measurements of PBAPs. These instruments have been applied in various
65 atmospheric environments, including rainforest (Gabey et al., 2010; Huffman et al., 2012),
66 forest (Huffman et al., 2013; Schumacher et al., 2013; Crawford et al., 2014), high-
67 altitude (Gabey et al., 2013; Valsan et al., 2016), rural (Healy et al., 2014), suburban
68 (Huffman et al., 2010; Toprak and Schnaiter, 2013) and urban environments (Gabey et al.,
69 2011; Miyakawa et al., 2015; Wei et al., 2016). Besides settled sampling sites, WIBS has
70 also been used for airborne observations (Perring et al., 2015). In clean environments,
71 these techniques can effectively distinguish PBAPs from other kinds of aerosol particles.
72 For example, Huffman et al. (2012) found similar size distributions of PBAPs measured
73 by UV-APS and scanning electron microscopy (SEM) in the Amazon rainforest.

74 PBAPs, however, are not the only fluorescent aerosol particles (FAPs) in the
75 atmosphere. Other materials such as polycyclic aromatic hydrocarbons (PAHs) and
76 humic-like substances (HULIS) may also fluoresce and contribute to the measured
77 fluorescence signals (Pöhlker et al., 2012). Hence, the fluorescent information given by
78 the instruments based on the fluorescence detection may include both fluorescent
79 biological and non-biological particles.

80 In order to have a deeper insight into the ambient FAPs in polluted area, we have
81 performed WIBS measurements in Nanjing, China in the autumn of 2013. In this study,
82 we first present the number concentration of FAPs in Nanjing in comparison to previous
83 studies. Then we demonstrate the potential impacts of combustion-related aerosol
84 particles in discrimination of bioaerosols under the polluted atmosphere. Finally, we
85 introduce alternative methods to quantify the relative contributions of different
86 fluorescent materials (combustion- and bioaerosol-type particles) to FAPs.

87 **2 Methods and instrumentation**

88 **2.1 Site description**

89 WIBS measurements were performed at the Station for Observing Regional
90 Processes of the Earth System (SORPES station), Xianlin campus of Nanjing University
91 (32.12 °N, 118.95 °E). Nanjing lies in the Yangtze River Delta with a total population of
92 8.18 million (data of 2013), and it's a large commercial center in the East China region.
93 The measurement site is ~20 km in the east of the urban center. The SORPES station is
94 located on a hill about 40 m above the surroundings. Details of this station were
95 described by Ding et al. (2013). [A 0.75 inch stainless-steel tube inlet was installed ~3 m](#)
96 [above the roof, and sample air was dried by a vertical silica gel drier prior to entering the](#)
97 [WIBS](#). Data were collected from 29 October to 15 November 2013.

98 **2.2 Instruments**

99 Measurements of FAPs were performed with a WIBS-4A. It uses the single-particle
100 elastic scattering intensity at 535 nm to calculate the optical size of particles. The
101 scattering signal is used to trigger the flash of two xenon lamps with UV wavelength of
102 280 nm and 370 nm, respectively. The fluorescent signals are recorded at two wavelength
103 bands (310-400 nm and 420-650 nm). This design results in three wavelength channels:
104 FL1 with excitation at 280 nm and detection 310–400 nm, FL2 with excitation
105 wavelength at 280 nm and detection wavelength at 420–650 nm, and FL3 with excitation
106 wavelength at 370 nm and detection wavelength at 420-650 nm. Respective abbreviations
107 are listed in Table 1. [During the measurement period, we used 1 μm and 2 μm fluorescent](#)
108 [and non-fluorescent PSL microspheres \(3K-990, B0100, 4K-02 and B0200, Duke](#)
109 [Scientific, Inc.\) for calibration](#). The fluorescence noise threshold is defined as:

$$110 \quad E_{\text{Threshold}} = E + 3\sigma \quad (1)$$

111 Where E is the modal baseline and σ is the standard deviations in each channel. Particles
112 with fluorescence signals above the noise threshold are classified as FAPs. Single-particle
113 data were converted into a size distribution with a 5-min integration time and particles
114 with diameter of 1-15 μm were analyzed in this study.

115 Meteorological data were collected with an Automatic Weather Station (CAMPBEL
116 co., AG1000). The differential mobility particle sizer (DMPS, built at Helsinki University)

117 was used to measure the number size distribution of sub-micron particles between 6 and
118 800 nm mobility diameter (Herrmann et al., 2014). Particle mass concentration below 0.8
119 μm ($PM_{0.8}$) was calculated from the measured size distributions assuming a density of 1.6
120 g cm^{-3} (Wang et al., 2014). A 7-wavelength “Spectrum” Aethalometer (AE-31, Magee
121 Scientific co.) was used to measure the black carbon (BC) mass concentration M_{BC} .

122 **3 Results and discussion**

123 **3.1 Non-biological fluorescent aerosol particles**

124 Figure 1 shows the time series of number concentrations and fractions of FAPs
125 during the measurement period. The number concentration of FAPs was dominated by
126 FL2 channel with a mean number concentration N_{FL2} of 3.4 cm^{-3} , followed by N_{FL3} of 2.1
127 cm^{-3} and N_{FL1} of 0.6 cm^{-3} . These number concentrations were 1~2 order of magnitudes
128 higher than those observed in clean areas where bioaerosols dominate the FAPs (Table 2).
129 For example, FAPs of 0.093 cm^{-3} , 0.15 cm^{-3} and 0.023 cm^{-3} were reported for the Amazon,
130 Borneo and Hyytiälä forests, respectively (Gabey et al., 2010; Huffman et al., 2012;
131 Toprak and Schnaiter, 2013). Since polluted areas are characterized by less plants and
132 natural biological processes, less bioaerosols are expected compared to the forests. This
133 much higher number concentration of FAPs observed in Nanjing suggests other kinds of
134 FAPs being detected by WIBS.

135 Previous studies (Pöhlker et al., 2012; Miyakawa et al., 2015; Perring et al., 2015)
136 reported that non-biological compounds like PAHs, mineral dust and HULIS can also
137 fluoresce. Several non-biological fluorophores such as SOAs, pyrene, humic acid and
138 naphthalene have fluorescent property in the same excitation and emission wavelength
139 bands of FL1 channel (Chang and Thompson, 2010; Pöhlker et al., 2012). These
140 materials originate from sources different from bioaerosols. For example, PAH enriches
141 on the surface of soot particles from biomass burning and fuel combustion, challenging
142 the interpretation of ambient particle fluorescence measurements.

143 Our sampling site is located in the vicinity of the polluted Nanjing city and is
144 intensively affected by human activities. To check the potential influences of PAH and
145 combustion processes, we compared the variability of FAPs with that of BC, on which
146 the PAHs are often coated. To minimize the impacts of transport and boundary layer

147 dynamics, we compared the ratio of BC and FAPs to the total particles in their respective
148 size range, i.e., $M_{BC}/PM_{0.8}$ and F_x instead of using absolute concentrations. Miyakawa et
149 al. (2015) used factor analysis based on carbon monoxide, elemental carbon and other
150 markers (using concentration instead of ratio) to identify "combustion-type" and "dust-
151 type" aerosols in urban areas. In our study, we found that $M_{BC}/PM_{0.8}$ showed a good
152 correlation with the number fraction of FAPs, especially in the FL1 channel ($r=0.748$,
153 Fig.1). For FL2 and FL3 channels, the number fractions also nicely followed the variation
154 of $M_{BC}/PM_{0.8}$ except for November 8, which deteriorated the overall correlation. Since
155 BC and PAHs are products of incomplete combustion, the similar variability suggests a
156 large contribution from combustion-related aerosols to the measured FAPs, especially in
157 FL1 channel. Our findings strongly support previous results (Toprak and Schnaiter, 2013;
158 Miyakawa et al., 2015) that FAPs (FL1 channel) may come from combustion process and
159 anthropogenic interference.

160 **3.2 Spectral patterns of fluorescent aerosol particles**

161 The complex nature of FAPs in polluted areas challenges the interpretation of
162 ambient measurements. Different fluorophores have their characteristic excitation-
163 emission matrices (EEM) map, which can be useful for discrimination of biological from
164 non-biological FAPs (Pöhlker et al., 2012). Since WIBS only has two excitation and
165 emission wavebands, a high-resolution EEM map cannot be retrieved. But we can still
166 consider the two wavebands as a low resolution EEMs, of which the distribution (i.e., the
167 ratio of the two wavebands) may also contain information about the nature of FAPs. For
168 example, we can assume two kinds of fluorescent compounds I and II have different
169 fluorescent spectra, as shown in Fig. 2a. For each compound, the integrated fluorescence
170 intensity are determined in two wavebands by WIBS (Fig. 2b). For qualitative analysis, a
171 normalized EEM is often used providing the relative wavelength dependence of
172 fluorescent materials. For WIBS, we simply used the ratio of fluorescence intensity from
173 different WIBS channels to represent the wavelength dependence (Fig. 2c).

174 Figure 3 shows the intensity distributions of aerosols particles in different
175 fluorescence bands/channels. Due to the instrument setting, fluorescence signal
176 intensities beyond 2200 arbitrary units (a.u.) are forced to the range of 2000-2200 a.u.,
177 regarding as saturated signal. Hence we only discussed fluorescence signal intensities

178 below 2000 a.u.. We first investigated the intensity ratio between channel FL1 and FL2,
179 as shown in Fig. 3a. With increasing fluorescence intensity, the number concentrations
180 sharply dropped, i.e., most of the abundant aerosol particles exhibited no or only weak
181 fluorescence. Using the intensity ratio of FL1 to FL2 (I_{FL1}/I_{FL2}) as a fluorescence
182 fingerprint, we obtained two prominent groups of aerosols with I_{FL1}/I_{FL2} approaching 0 or
183 infinity. $I_{FL1}/I_{FL2} \sim 0$ means that the aerosol have a low FL1 intensity below the detection
184 limit and a high FL2 intensity, while I_{FL1}/I_{FL2} approaching infinity means the opposite.
185 According to the detection thresholds of both FL1 and FL2 channels, we then classified
186 the aerosol particles into four groups with FL1/FL2 above or below the detection
187 threshold (labelled as g1 to g4 in Fig. 3). We further investigated the FL3 properties of
188 the various groups. As shown in Figs. 3b-3d, the aerosol number concentration decreased
189 as FL3 intensity increased resembling the distribution for FL1 and FL2. Similarly we
190 used the fluorescence threshold of FL3 to classify aerosols from g1 to g4 into subgroups.

191 Our efforts towards a spectral fingerprint resulted in the same classification method
192 as in Perring et al. (2015). Here we adopted the labels of Perring et al. (2015) in which
193 channel A refers to FL1, channel B refers to FL2 and channel C refers to FL3. Any
194 aerosol particle can have signals above/below the fluorescence threshold in any of these
195 channels, leading to seven combinations of fluorescence signals, i.e., particles with
196 fluorescence signals above the threshold in single channel as types A, B and C; particles
197 with fluorescence signals in two channels as types AB, AC and BC and particles with
198 fluorescence signals in all three channels as type ABC (Table 1).

199 As shown in Fig.4a, types B, BC and C were the most abundant FAPs, followed by
200 types ABC, AB and A. Type AC had the lowest loading and was not even visible. The
201 mean number concentrations of dominant types B, BC and C were 1.77 cm^{-3} , 1.06 cm^{-3}
202 and 0.66 cm^{-3} , respectively (Table 3). The number concentration of 7-type FAPs
203 exhibited strong diurnal and day-to-day variability (Fig. 5). Number concentration of
204 FAPs peaked in the morning (~08:00 local time) and reached a minimum in the afternoon
205 (~14:00). Their similar diurnal patterns indicate the dominant effect of boundary layer
206 development in controlling the variability of aerosol particles, which was also shown in
207 FL1, FL2 and FL3 channels (Figure S1). To better understand the source of FAPs, we
208 also investigated the number fraction of FAPs in total particles. The boundary layer

209 development exerts similar effect on all kinds of aerosol particles. Thus for particles of
210 the same origin, their ratios will remain constant and a difference in their ratios reflects
211 their different sources. As shown in Fig. 5, the fractions of FAPs presented quite different
212 diurnal patterns. The fractions of type BC revealed substantial diurnal opposite with a
213 clear morning peak and early afternoon minimum. Type A and type B showed a much
214 weaker variability, implying a similar source of FAPs as the total aerosol particles.

215 The number size distributions of FAPs were shown in Figure 6. The highest FAPs
216 number concentration came out at $\sim 1 \mu\text{m}$ except type ABC. Type ABC peaked at 1-2 μm
217 with a second peak at 4-6 μm . For type A, type C and type BC the number concentration
218 monotonously decreased with size increased. No fluorescence signals were found in FL1
219 and FL3 channels (corresponding to type A, type C and type AC FAPs) for the particles
220 of size larger than 4 μm . On the contrary, the number fractions of FAPs generally
221 increased as the particle size increased, reaching $\sim 100\%$ at 3-4 μm for FL2 channel (not
222 shown in Fig.6). These results reveal that most coarse mode particles contain certain
223 kinds of fluorophores.

224 Meanwhile, we compared the number fraction of 7-type FAPs with $M_{\text{BC}}/PM_{0.8}$, the
225 results indicate that the number fractions of types A, AB, and ABC showed good
226 correlations with $M_{\text{BC}}/PM_{0.8}$ (Fig. 7), suggesting a large contribution of combustion-
227 related aerosol particles to these types. Note that all these types contain FL1 signals,
228 implying the potential application of FL1 in the identification of biomass burning (or
229 other combustions) events. Likewise, fluorescent types B and BC mostly followed the
230 variation of $M_{\text{BC}}/PM_{0.8}$ except for November 8 when elevated fractional contributions
231 were observed one day before a rain event on November 9. A dramatic release of certain
232 fungal spores was often observed before rain (Hjelmroos, 1993). However, the increase
233 on November 8 was mainly contributed by 1-2 μm FAPs rather than fungal spores (> 3
234 μm) shown by Hjelmroos (1993). So the origin of this elevated FAPs remained
235 inconclusive. Moreover, good correlation ($r=0.58$) between type B particles in 3-4 μm
236 and $M_{\text{BC}}/PM_{0.8}$, suggesting a closer link of this peak with type B particles to combustion
237 process. Fluorescent type C showed a weak negative correlation with $M_{\text{BC}}/PM_{0.8}$,
238 suggesting a minor role of combustion-related aerosols or major contribution of non-
239 combustion related aerosols (e.g., bioaerosols or dusts).

240 3.3 Fluorescence intensity

241 Besides the relative wavelength dependence, the absolute quantum yield is also one
242 of the most important characteristics of a fluorophore. Discrepancies in the quantum yield
243 can directly influence the fluorescence, resulting in different intensity levels. Thus it is
244 possible to use the intensity information to identify different kinds of FAPs. Huffman et
245 al. (2012) showed that the UV-APS can be used to successfully discriminate bioaerosols
246 from dust particles, both of which have been suggested to fluoresce (Pöhlker et al., 2012).

247 We first made a hypothesis that there exists a characteristic intensity value I_{cri} , above
248 which most FAPs are bioaerosols. Since I_{cri} cannot be directly inferred from the intensity
249 distribution (Fig. 3), we adopted the parameter $M_{\text{BC}}/PM_{0.8}$ to assist our analysis. This is
250 because bioaerosols and combustion-related FAPs are of different origins, we scanned
251 different values for I_{cri} until the corresponding FAPs (of intensity $> I_{\text{cri}}$) fraction showed a
252 non-positive correlation with $M_{\text{BC}}/PM_{0.8}$. In this study, we mainly focus on the FL3
253 channel since it is running in a similar excitation-emission wavelength as the UV-APS
254 and it has been validated against other independent method. We thereby suggest that FL3
255 channel can be used to discriminate bioaerosols from combustion-generated FAPs in a
256 similar approach. The analysis of FL1 and FL2 channels were shown in the
257 supplementary Information (Figure S2 and Figure S3). Figure 8 shows the averaged
258 fractional contribution of FAPs with $I_{\text{FL3}} > I_{\text{cri}}$ at different $M_{\text{BC}}/PM_{0.8}$ levels. To account
259 for the size dependence of fluorescence signals, we first classified FAPs according to the
260 particle size. For the 1-2 μm size range, the fraction was always positively correlated
261 with $M_{\text{BC}}/PM_{0.8}$ and was independent of the selection of I_{cri} . For the size range of 2-5 μm ,
262 the FAPs showed mostly negative correlation with $M_{\text{BC}}/PM_{0.8}$ and were also independent
263 of the I_{cri} selection. For FAPs larger than 5 μm , the selection of I_{cri} became critical. With
264 increasing I_{cri} , the dependence of FL3 fraction on $M_{\text{BC}}/PM_{0.8}$ gradually became weaker
265 and finally turned to negative at $I_{\text{cri}} > 40$ a.u.. The results at 5-15 μm were consistent with
266 our hypothesis that bioaerosols have stronger fluorescence intensity than combustion-
267 related aerosol particles and can be discriminated from their fluorescence intensity. The
268 different correlation statistics of 1-2 μm and 2-5 μm may be explained by the different
269 abundance of bioaerosols and combustion-related aerosols at different size range. The 2-5
270 μm mode was dominated by bioaerosols, while the 1-2 μm mode was dominated by

271 combustion-related aerosol particles. Therefore there was no clear dependence on the
272 selection of I_{cri} . Saari et al. (2015) reported that FAPs at 0.5-1.5 μm might be due to
273 anthropogenic emissions such as biomass burning, while most fungal spores and pollen
274 dominated the larger size range (Despr es et al., 2012). It is also possible that I_{cri} had a
275 size dependence because different types of bioaerosols may dominate different size
276 ranges.

277 By integrating the FAPs of different correlations with $M_{\text{BC}}/PM_{0.8}$, we retrieved the
278 number concentrations of “non-combustion-related” (NCR) type particles (FAPs with
279 $I_{\text{FL3}} > 18$ a.u. at 2-5 μm and FAPs with $I_{\text{FL3}} > 40$ a.u. at 5-15 μm) and “combustion-related”
280 (CR) type particles (FAPs with $I_{\text{FL3}} > 18$ a.u. at 1-2 μm and FAPs with $40 \geq I_{\text{FL3}} > 18$ a.u. at
281 5-15 μm). The mean number concentrations of NCR type and CR type particles were
282 $0.64 \pm 0.46 \text{ cm}^{-3}$ and $1.45 \pm 1.06 \text{ cm}^{-3}$, respectively. The NCR type FAPs are likely
283 bioaerosols.

284 In this study, we applied two methods to classify FAPs measured by WIBS,
285 resulting in two non-combustion-types of particles: type C particles derived from
286 fluorescent spectral pattern analysis and NCR type particles derived from fluorescence
287 intensity pattern analysis. As shown in Table 3, the mean number concentrations of type
288 C and NCR type particle were 0.66 cm^{-3} and 0.64 cm^{-3} , which were still higher than those
289 found in PBAPs-dominated regions like the Amazon (Huffman et al., 2012), Hyyti l 
290 (Schumacher et al., 2013) and PdD (Gabey et al., 2013). This indicates that still a residual
291 of these non-combustion type particles may comprise other fluorescent constituents like
292 mineral dusts (Miyakawa et al., 2015; Perring et al., 2015).

293 **4. Conclusions**

294 On-line measurements of FAPs have been performed in Nanjing by using WIBS in
295 the autumn of 2013. Our results showed that the number concentrations of FAPs were
296 1~2 order of magnitudes higher than those reported in the previous studies. The observed
297 high values suggested that directly using FL1, FL2 and FL3 channels to index PBAPs is
298 not suitable for polluted areas. The number fraction of FL1 showed strong correlation
299 with $M_{\text{BC}}/PM_{0.8}$ ($r=0.748$), indicative of a strong bias by anthropogenic emissions.

300 In this study, we used two methods to classify the FAPs. According to the threshold
301 of each channel, FAPs were divided into 7 types. Number fraction of type C showed
302 negative correlation ($r=-0.13$) with $M_{BC}/PM_{0.8}$, which might be more representative for
303 bioaerosols. Meanwhile, on the basis of the FL3 fluorescent intensity and its correlations
304 with $M_{BC}/PM_{0.8}$, FL3 fluorescent particles were divided into 2 types. Combustion-related
305 type particles seemed to dominate 1-2 μm , while the non-combustion-related type
306 particles, which concentrated in the size range of 2-5 μm and showed negative correlation
307 ($r=-0.121$) with $M_{BC}/PM_{0.8}$, might be originated from biological emissions. The number
308 concentrations of the identified two types of bioaerosols (0.66 cm^{-3} for type C particles
309 and 0.64 cm^{-3} for non-combustion-related type), however, were still higher than those
310 observed in clean background areas and previous study in Nanjing (Wei et al., 2015),
311 indicating they may also include some other fluorophores, such as dusts.

312 Our results suggested that fluorescence measurements in polluted areas are prone to
313 interferences and uncertainty introduced by the anthropogenic emissions. Discrimination
314 of biological particles from FAPs still needs further development. Each fluorophore
315 species presents unique fluorescence spectrum, hence we can effectively distinguish
316 biological particles from other FAPs based on their specific EEM maps. Due to the
317 limitation of excitation and emission wavebands of WIBS, the development of a multi-
318 wavebands instrument is hence needed. Other methods such as the cluster analysis
319 (Robinson et al., 2013; Crawford et al., 2014; Crawford et al., 2015) also exhibited the
320 ability to differentiate various FAPs. Measuring additional particle properties such as size
321 and morphology will help ameliorate the interferences by providing additional
322 dimensions to distinguish fluorescent particles of different emission mechanisms.

323 **Acknowledgments**

324 This study was supported by the Max Plank Society (MPG), the European Commission
325 under the projects BACCHUS (Grant No. 603445) and the Natural Science Foundation of
326 China (Project No. 91544103). Xiawei Yu and Minghui Zhang would like to thank the
327 China Scholarship Council (CSC) for financial support. We thank the SORPES-NJU
328 station for logistic and instrumentation support.
329

330 References

- 331 Bary, A., Garnsey, H. E. F., and Balfour, I. B.: Comparative morphology and biology of the fungi,
332 mycetoza and bacteria, Clarendon Press, 1887.
- 333 Brosseau, L. M., Vesley, D., Rice, N., Goodell, K., Nellis, M., and Hairston, P.: Differences in
334 Detected Fluorescence Among Several Bacterial Species Measured with a Direct-Reading
335 Particle Sizer and Fluorescence Detector, *Aerosol Sci. Technol.*, 32, 545-558,
336 10.1080/027868200303461, 2000.
- 337 Cao, C., Jiang, W., Wang, B., Fang, J., Lang, J., Tian, G., Jiang, J., and Zhu, T. F.: Inhalable
338 Microorganisms in Beijing's PM_{2.5} and PM₁₀ Pollutants during a Severe Smog Event, *Environ*
339 *Sci Technol*, 48, 1499-1507, 10.1021/es4048472, 2014.
- 340 Chang, J. L., and Thompson, J. E.: Characterization of colored products formed during irradiation
341 of aqueous solutions containing H₂O₂ and phenolic compounds, *Atmos. Environ.*, 44, 541-551,
342 2010.
- 343 Christner, B. C., Morris, C. E., Foreman, C. M., Cai, R., and Sands, D. C.: Ubiquity of Biological
344 Ice Nucleators in Snowfall, *Science*, 319, 1214, 10.1126/science.1149757, 2008.
- 345 Crawford, I., Robinson, N. H., Flynn, M. J., Foot, V. E., Gallagher, M. W., Huffman, J. A.,
346 Stanley, W. R., and Kaye, P. H.: Characterisation of bioaerosol emissions from a Colorado pine
347 forest: results from the BEACHON-RoMBAS experiment, *Atmos Chem Phys*, 14, 8559-8578,
348 10.5194/acp-14-8559-2014, 2014.
- 349 Crawford, I., Ruske, S., Topping, D. O., and Gallagher, M. W.: Evaluation of hierarchical
350 agglomerative cluster analysis methods for discrimination of primary biological aerosol, *Atmos.*
351 *Meas. Tech.*, 8, 4979-4991, 10.5194/amt-8-4979-2015, 2015.
- 352 Creamean, J. M., Suski, K. J., Rosenfeld, D., Cazorla, A., DeMott, P. J., Sullivan, R. C., White, A.
353 B., Ralph, F. M., Minnis, P., Comstock, J. M., Tomlinson, J. M., and Prather, K. A.: Dust and
354 Biological Aerosols from the Sahara and Asia Influence Precipitation in the Western U.S, *Science*,
355 339, 1572-1578, 10.1126/science.1227279, 2013.
- 356 DeLeon-Rodriguez, N., Latham, T. L., Rodriguez-R, L. M., Barazesh, J. M., Anderson, B. E.,
357 Beyersdorf, A. J., Ziemba, L. D., Bergin, M., Nenes, A., and Konstantinidis, K. T.: Microbiome
358 of the upper troposphere: Species composition and prevalence, effects of tropical storms, and
359 atmospheric implications, *P Natl Acad Sci USA*, 10.1073/pnas.1212089110, 2013.
- 360 Despré, V. R., Huffman, J. A., Burrows, S. M., Hoose, C., Safatov, A. S., Buryak, G., Fröhlich-
361 Nowoisky, J., Elbert, W., Andreae, M. O., Pöschl, U., and Jaenicke, R.: Primary biological
362 aerosol particles in the atmosphere: a review, *Tellus B*, 64, 2012.
- 363 Ding, A. J., Fu, C. B., Yang, X. Q., Sun, J. N., Zheng, L. F., Xie, Y. N., Herrmann, E., Nie, W.,
364 Petäjä T., Kerminen, V. M., and Kulmala, M.: Ozone and fine particle in the western Yangtze
365 River Delta: an overview of 1 yr data at the SORPES station, *Atmos Chem Phys*, 13, 5813-5830,
366 10.5194/acp-13-5813-2013, 2013.
- 367 Duchaine, C., Thorne, P. S., Mériaux, A., Grimard, Y., Whitten, P., and Cormier, Y.: Comparison
368 of endotoxin exposure assessment by bioaerosol impinger and filter-sampling methods, *Appl.*
369 *Environ. Microbiol.*, 67, 2775-2780, 2001.
- 370 Gabey, A. M., Gallagher, M. W., Whitehead, J., Dorsey, J. R., Kaye, P. H., and Stanley, W. R.:
371 Measurements and comparison of primary biological aerosol above and below a tropical forest
372 canopy using a dual channel fluorescence spectrometer, *Atmos Chem Phys*, 10, 4453-4466,
373 10.5194/acp-10-4453-2010, 2010.
- 374 Gabey, A. M., Stanley, W. R., Gallagher, M. W., and Kaye, P. H.: The fluorescence properties of
375 aerosol larger than 0.8 μm in urban and tropical rainforest locations, *Atmos Chem Phys*, 11,
376 5491-5504, 10.5194/acp-11-5491-2011, 2011.
- 377 Gabey, A. M., Vaitilingom, M., Freney, E., Boulon, J., Sellegri, K., Gallagher, M. W., Crawford,
378 I. P., Robinson, N. H., Stanley, W. R., and Kaye, P. H.: Observations of fluorescent and

379 biological aerosol at a high-altitude site in central France, *Atmos Chem Phys*, 13, 7415-7428,
380 10.5194/acp-13-7415-2013, 2013.

381 Griffin, D. W.: Atmospheric movement of microorganisms in clouds of desert dust and
382 implications for human health, *Clin. Microbiol. Rev.*, 20, 459-477, Doi 10.1128/Cmr.00039-06,
383 2007.

384 Haldane, J., and Anderson, A.: The carbonic acid, organic matter, and micro-organisms in air,
385 more especially of dwellings and schools, *Philosophical Transactions of the Royal Society of*
386 *London. B*, 61-111, 1887.

387 Hallar, A. G., Chirokova, G., McCubbin, I., Painter, T. H., Wiedinmyer, C., and Dodson, C.:
388 Atmospheric bioaerosols transported via dust storms in the western United States, *Geophys. Res.*
389 *Let.*, 38, L17801, 10.1029/2011GL048166, 2011.

390 Healy, D. A., Huffman, J. A., O'Connor, D. J., Pöhlker, C., Pöschl, U., and Sodeau, J. R.:
391 Ambient measurements of biological aerosol particles near Killarney, Ireland: a comparison
392 between real-time fluorescence and microscopy techniques, *Atmos Chem Phys*, 14, 8055-8069,
393 10.5194/acp-14-8055-2014, 2014.

394 Henningson, E. W., and Ahlberg, M. S.: Evaluation of microbiological aerosol samplers: a review,
395 *J. Aerosol Sci.*, 25, 1459-1492, 1994.

396 Herrmann, E., Ding, A. J., Kerminen, V. M., Petäjä T., Yang, X. Q., Sun, J. N., Qi, X. M.,
397 Manninen, H., Hakala, J., Nieminen, T., Aalto, P. P., Kulmala, M., and Fu, C. B.: Aerosols and
398 nucleation in eastern China: first insights from the new SORPES-NJU station, *Atmos Chem Phys*,
399 14, 2169-2183, 10.5194/acp-14-2169-2014, 2014.

400 Hjelmroos, M.: Relationship between airborne fungal spore presence and weather variables:
401 *Cladosporium* and *Alternaria*, *Grana*, 32, 40-47, 1993.

402 Huffman, J. A., Treutlein, B., and Pöschl, U.: Fluorescent biological aerosol particle
403 concentrations and size distributions measured with an Ultraviolet Aerodynamic Particle Sizer
404 (UV-APS) in Central Europe, *Atmos Chem Phys*, 10, 3215-3233, 10.5194/acp-10-3215-2010,
405 2010.

406 Huffman, J. A., Sinha, B., Garland, R. M., Snee-Pollmann, A., Gunthe, S. S., Artaxo, P., Martin,
407 S. T., Andreae, M. O., and Pöschl, U.: Size distributions and temporal variations of biological
408 aerosol particles in the Amazon rainforest characterized by microscopy and real-time UV-APS
409 fluorescence techniques during AMAZE-08, *Atmos Chem Phys*, 12, 11997-12019, 10.5194/acp-
410 12-11997-2012, 2012.

411 Huffman, J. A., Prenni, A. J., DeMott, P. J., Pöhlker, C., Mason, R. H., Robinson, N. H.,
412 Fröhlich-Nowoisky, J., Tobo, Y., Després, V. R., Garcia, E., Gochis, D. J., Harris, E., Müller-
413 Germann, I., Ruzene, C., Schmer, B., Sinha, B., Day, D. A., Andreae, M. O., Jimenez, J. L.,
414 Gallagher, M., Kreidenweis, S. M., Bertram, A. K., and Pöschl, U.: High concentrations of
415 biological aerosol particles and ice nuclei during and after rain, *Atmos Chem Phys*, 13, 6151-
416 6164, 10.5194/acp-13-6151-2013, 2013.

417 Miyakawa, T., Kanaya, Y., Taketani, F., Tabaru, M., Sugimoto, N., Ozawa, Y., and Takegawa, N.:
418 Ground-based measurement of fluorescent aerosol particles in Tokyo in the spring of 2013:
419 Potential impacts of nonbiological materials on autofluorescence measurements of airborne
420 particles, *J. Geophys. Res. Atmos.*, 120, 1171-1185, 10.1002/2014jd022189, 2015.

421 Morris, C. E., Sands, D. C., Glaux, C., Samsatly, J., Asaad, S., Moukamel, A. R., Gonçalves, F. L.
422 T., and Bigg, E. K.: Urediospores of rust fungi are ice nucleation active at > -10 °C and harbor
423 ice nucleation active bacteria, *Atmos Chem Phys*, 13, 4223-4233, 10.5194/acp-13-4223-2013,
424 2013.

425 Oliver, J. D.: The viable but nonculturable state in bacteria, *J Microbiol*, 43, 93-100, 2005.

426 Pan, Y.-L., Pinnick, R. G., Hill, S. C., and Chang, R. K.: Particle-Fluorescence Spectrometer for
427 Real-Time Single-Particle Measurements of Atmospheric Organic Carbon and Biological Aerosol,
428 *Environ. Sci. Technol.*, 43, 429-434, 10.1021/es801544y, 2009.

429 Perring, A. E., Schwarz, J. P., Baumgardner, D., Hernandez, M. T., Spracklen, D. V., Heald, C. L.,
430 Gao, R. S., Kok, G., McMeeking, G. R., McQuaid, J. B., and Fahey, D. W.: Airborne
431 observations of regional variation in fluorescent aerosol across the United States, *J Geophys Res-*
432 *Atmos*, 120, 1153-1170, 10.1002/2014JD022495, 2015.

433 Pöhlker, C., Huffman, J. A., and Pöschl, U.: Autofluorescence of atmospheric bioaerosols –
434 fluorescent biomolecules and potential interferences, *Atmos. Meas. Tech.*, 5, 37-71, 10.5194/amt-
435 5-37-2012, 2012.

436 Polymenakou, P. N., Mandalakis, M., Stephanou, E. G., and Tselepidis, A.: Particle size
437 distribution of airborne microorganisms and pathogens during an intense African dust event in the
438 eastern Mediterranean, *Environ. Health Perspect.*, 116, 292-296, Doi 10.1289/Ehp.10684, 2008.

439 Pöschl, U.: Atmospheric aerosols: Composition, transformation, climate and health effects,
440 *Angewandte Chemie-International Edition*, 44, 7520-7540, DOI 10.1002/anie.200501122, 2005.

441 Pöschl, U., Martin, S. T., Sinha, B., Chen, Q., Gunthe, S. S., Huffman, J. A., Borrmann, S.,
442 Farmer, D. K., Garland, R. M., Helas, G., Jimenez, J. L., King, S. M., Manzi, A., Mikhailov, E.,
443 Pauliquevis, T., Petters, M. D., Prenni, A. J., Roldin, P., Rose, D., Schneider, J., Su, H., Zorn, S.
444 R., Artaxo, P., and Andreae, M. O.: Rainforest Aerosols as Biogenic Nuclei of Clouds and
445 Precipitation in the Amazon, *Science*, 329, 1513-1516, 10.1126/science.1191056, 2010.

446 Robinson, N. H., Allan, J. D., Huffman, J. A., Kaye, P. H., Foot, V. E., and Gallagher, M.:
447 Cluster analysis of WIBS single-particle bioaerosol data, *Atmos. Meas. Tech.*, 6, 337-347,
448 10.5194/amt-6-337-2013, 2013.

449 Saari, S., Niemi, J., Rönkkö, T., Kuuluvainen, H., Järvinen, A., Pirjola, L., Aurela, M., Hillamo,
450 R., and Keskinen, J.: Seasonal and Diurnal Variations of Fluorescent Bioaerosol Concentration
451 and Size Distribution in the Urban Environment, *Aerosol and Air Quality Research*, 15, 572-581,
452 2015.

453 Schumacher, C. J., Pöhlker, C., Aalto, P., Hiltunen, V., Petäjä, T., Kulmala, M., Pöschl, U., and
454 Huffman, J. A.: Seasonal cycles of fluorescent biological aerosol particles in boreal and semi-arid
455 forests of Finland and Colorado, *Atmos Chem Phys*, 13, 11987-12001, 10.5194/acp-13-11987-
456 2013, 2013.

457 Taketani, F., Kanaya, Y., Nakamura, T., Koizumi, K., Moteki, N., and Takegawa, N.:
458 Measurement of fluorescence spectra from atmospheric single submicron particle using laser-
459 induced fluorescence technique, *J. Aerosol Sci.*, 58, 1-8,
460 <http://dx.doi.org/10.1016/j.jaerosci.2012.12.002>, 2013.

461 Toprak, E., and Schnaiter, M.: Fluorescent biological aerosol particles measured with the
462 Waveband Integrated Bioaerosol Sensor WIBS-4: laboratory tests combined with a one year field
463 study, *Atmos Chem Phys*, 13, 225-243, 10.5194/acp-13-225-2013, 2013.

464 Valsan, A. E., Ravikrishna, R., Biju, C. V., Pöhlker, C., Despré, V. R., Huffman, J. A., Pöschl,
465 U., and Gunthe, S. S.: Fluorescent Biological Aerosol Particle Measurements at a Tropical High
466 Altitude Site in Southern India during Southwest Monsoon Season, *Atmos. Chem. Phys. Discuss.*,
467 2016, 1-80, 10.5194/acp-2016-265, 2016.

468 Wang, H., Zhu, B., Shen, L., Liu, X., Zhang, Z., and Yang, Y.: Size distributions of aerosol
469 during the Spring Festival in Nanjing, *Huan jing ke xue (in Chinese)*, 35, 442-450, 2014.

470 Wei, K., Zheng, Y., Li, J., Shen, F., Zou, Z., Fan, H., Li, X., Wu, C.-y., and Yao, M.: Microbial
471 aerosol characteristics in highly polluted and near-pristine environments featuring different
472 climatic conditions, *Science Bulletin*, 60, 1439-1447, 10.1007/s11434-015-0868-y, 2015.

473 Wei, K., Zou, Z., Zheng, Y., Li, J., Shen, F., Wu, C.-y., Wu, Y., Hu, M., and Yao, M.: Ambient
474 bioaerosol particle dynamics observed during haze and sunny days in Beijing, *Sci. Total Environ.*,
475 550, 751-759, <http://dx.doi.org/10.1016/j.scitotenv.2016.01.137>, 2016.

476 Yu, J., Hu, Q., Xie, Z., Kang, H., Li, M., Li, Z., and Ye, P.: Concentration and Size Distribution
477 of Fungi Aerosol over Oceans along a Cruise Path during the Fourth Chinese Arctic Research
478 Expedition, *Atmosphere*, 4, 337-348, 2013.

479

480

481 **Tables**482 **Table 1.** Definition of abbreviations used in the text.

Short name	Description
PBAPs	Primary biological aerosol particles
FAPs	Fluorescent aerosol particles
FL1	Fluorescent detected in channel F1 280 (excitation at 280 nm, detection 310–400 nm)
FL2	Fluorescent detected in channel F2 280 (excitation at 280 nm, detection 420–650 nm)
FL3	Fluorescent detected in channel F2 370 (excitation at 370 nm, detection 420–650 nm)
Type A	Fluorescent particle signal in channel FL1 only
Type B	Fluorescent particle signal in channel FL2 only
Type C	Fluorescent particle signal in channel FL3 only
Type AB	Fluorescent particle signal in channels FL1 and FL2
Type AC	Fluorescent particle signal in channels FL1 and FL3
Type BC	Fluorescent particle signal in channels FL2 and FL3
Type ABC	Fluorescent particle signal in channels FL1, FL2 and FL3
N_x	Number concentration of each type particles
F_x	Number fraction of each type particles
M_{BC}	Mass concentration of black carbon
$PM_{0.8}$	Mass concentration of particles in the size range of 0.006-0.8 μm
D_o	Particle optical equivalent diameter
a.u.	Arbitrary units

484 **Table 2.** Comparisons between the results of this study and previous studies. Unit for the number concentration of fluorescent
 485 particles is L^{-1} . Numbers in brackets are the number fractions of fluorescent particles (%).

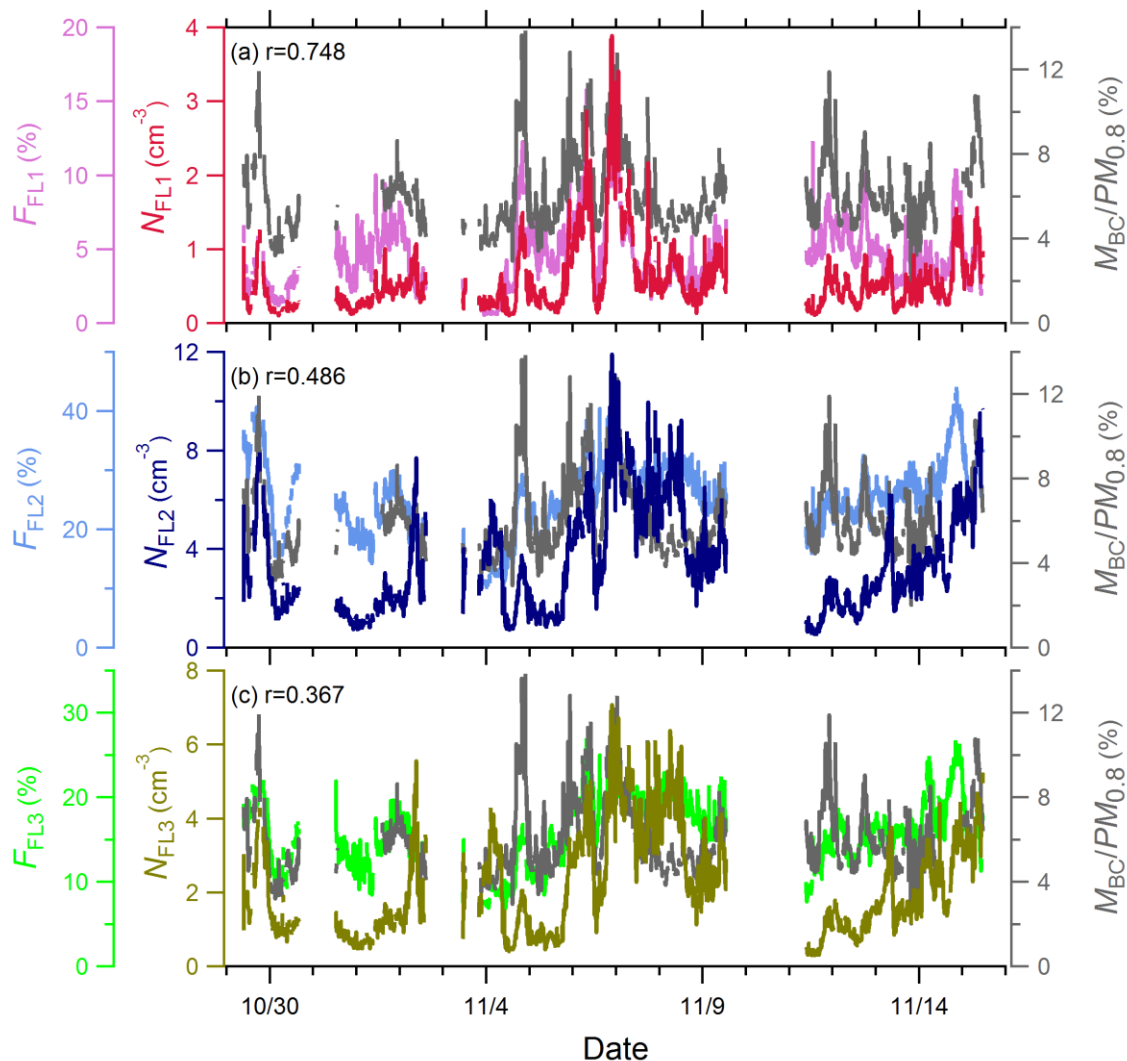
Site Location	Site Category	Season	N_{FL1}	N_{FL2}	N_{FL3}	N_{FAPs}	References
Nanjing, China	sub-urban	autumn	570 (4.6)	3350 (25.3)	2090 (15.6)	-	This study
Manchester, UK	urban	winter	29 (2.1)	52 (3.7)	110 (7.8)	-	(Gabey et al., 2011)
Puy de Dôme mountain, France	high-altitude	summer	12 (4.4)	-	95 (35.2)	-	(Gabey et al., 2013)
Killarney, Ireland	rural	summer	175 (0.5)	95 (0.3)	35 (0.1)	15 (0.05) ^a	(Healy et al., 2014)
Borneo, Malaysia	rainforest	summer	-	-	-	150 ^b	(Gabey et al., 2010)
Karlsruhe, Germany	semi-rural	one year	-	-	-	31 (7.3) ^b	(Toprak and Schnaiter, 2013)
Amazon, Brazil	rainforest	spring	-	-	-	93 (26.3) ^a	(Huffman et al., 2012)
Mainz, Germany	semi-urban	summer, autumn, winter	-	-	-	27 (4) ^a	(Huffman et al., 2010)
Helsinki, Finland	urban	summer	-	-	-	13 (8) ^a	(Saari et al., 2015)
		spring	-	-	-	15 (4.4) ^a	
Hyytiälä, Finland	boreal forest	summer	-	-	-	46 (13) ^a	(Schumacher et al., 2013)
		autumn	-	-	-	27 (9.8) ^a	
		winter	-	-	-	4 (1.1) ^a	
		spring	-	-	-	15 (2.5) ^a	
Colorado, USA	rural	summer	-	-	-	30 (8.8) ^a	(Schumacher et al., 2013)
		autumn	-	-	-	17 (5.7) ^a	
		winter	-	-	-	5.3 (3) ^a	
Ghats, India	high-altitude	summer	-	-	-	20 (2) ^a	(Valsan et al., 2016)

486 a: results of UV-APS;

487 b: combine with FL1 and FL3 channel

488 **Table 3.** Integrated number concentrations (cm^{-3}) of each FAPs and fractions (%) of
 489 FAPs number concentrations to the total particle number concentration. Type AC is not
 490 listed.

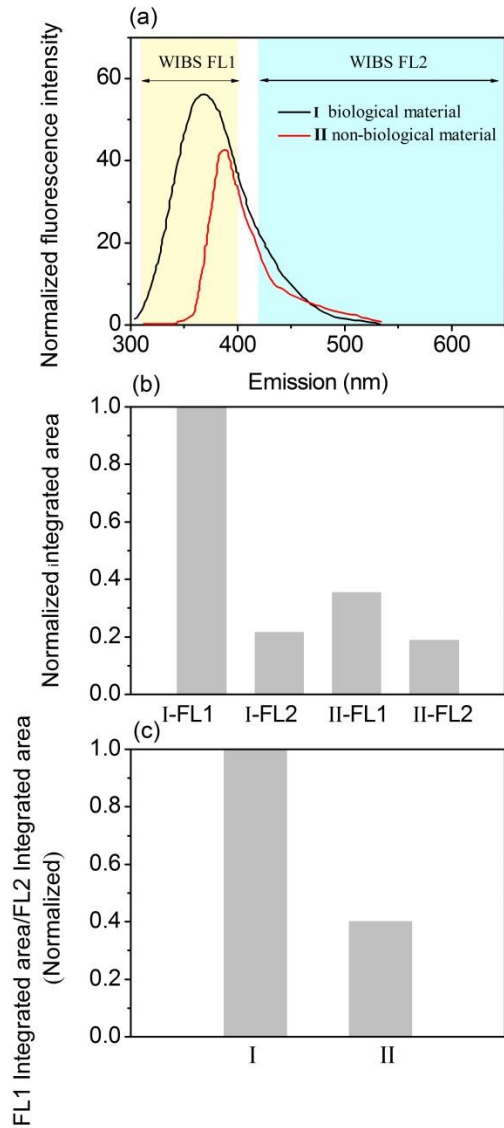
Category	25th Percentile	Mean	Median	75th Percentile	Standard Deviation	Fraction
Type A	0.03	0.05	0.04	0.06	0.03	0.45
Type B	0.79	1.77	1.42	2.55	1.27	12.95
Type C	0.23	0.66	0.43	0.95	0.55	4.40
Type AB	0.07	0.15	0.11	0.18	0.12	1.20
Type BC	0.52	1.06	0.87	1.51	0.73	8.26
Type ABC	0.17	0.37	0.28	0.43	0.31	2.91
CR type	0.63	1.45	1.10	2.11	1.06	10.50
NCR type	0.32	0.64	0.54	0.83	0.46	4.69



492

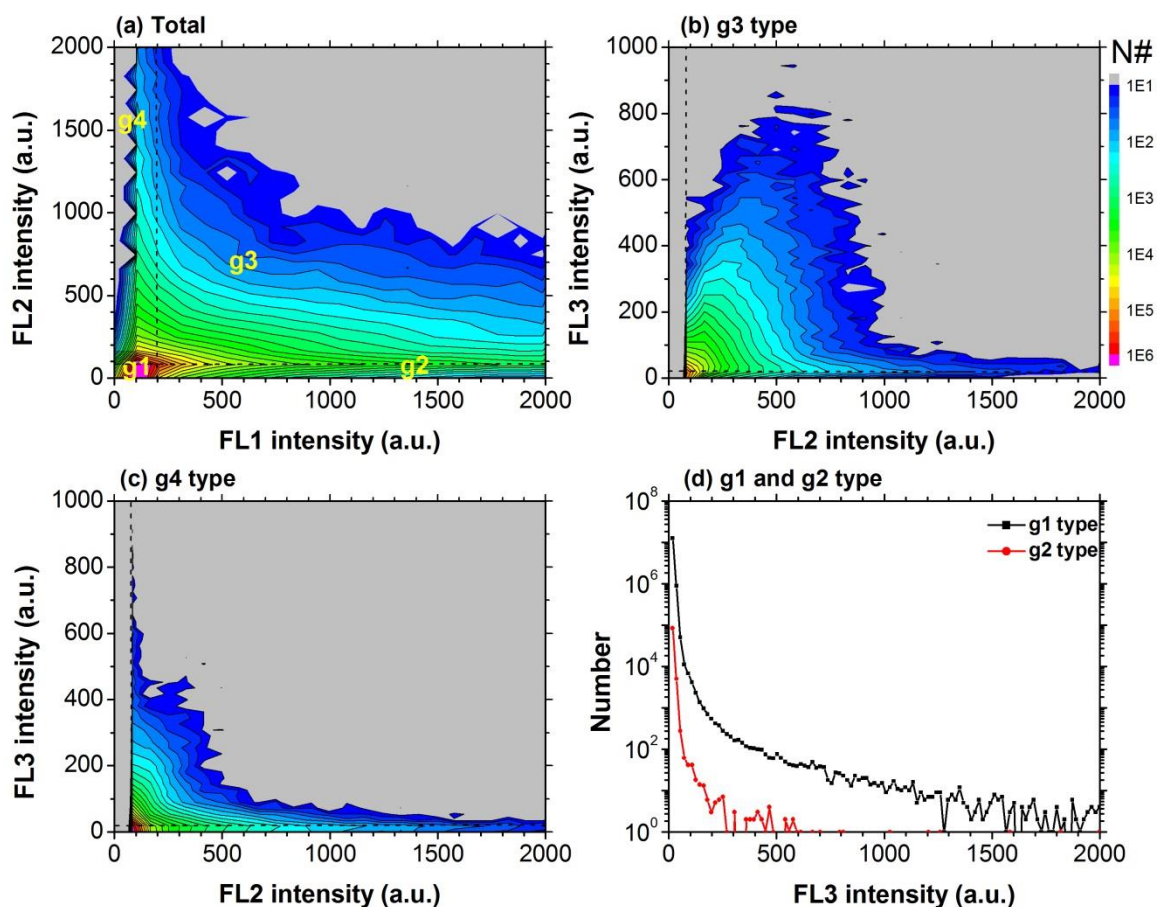
493 Figure 1. Time series of $M_{BC}/PM_{0.8}$ (gray line, right axis), number concentration of
 494 fluorescent particles in each channel (primary left axis) and relative number fractions of
 495 fluorescent particles in each channel (secondary left axis). (a) FL1 channel, N_{FL1} , crimson
 496 line, F_{FL1} , orchid line. (b) FL2 channel, N_{FL2} , navy line F_{FL2} , cornflower blue line. (c) FL3
 497 channel, N_{FL3} , olive line F_{FL3} , lime line. r is the correlation coefficient between F_x and
 498 $M_{BC}/PM_{0.8}$.

499



500

501 **Figure 2.** (a) Normalized fluorescence emission spectra of two fluorescent compounds: I
 502 (black line, biological material) and II (red line, non-biological material) for excitation
 503 wavelengths at $\lambda_{ex}=280$ nm. Shadow areas indicate the excitation wavebands of FL1 and
 504 FL2 channels of WBS. (b) Integrated fluorescence intensity of two compounds in two
 505 bands (FL1 and FL2). (c) The ratio of fluorescence intensity from different WBS
 506 channels (I_{FL1}/I_{FL2}) of I and II compounds. The fluorescence emission spectra are
 507 obtained from Pöhlker et al. (2012).

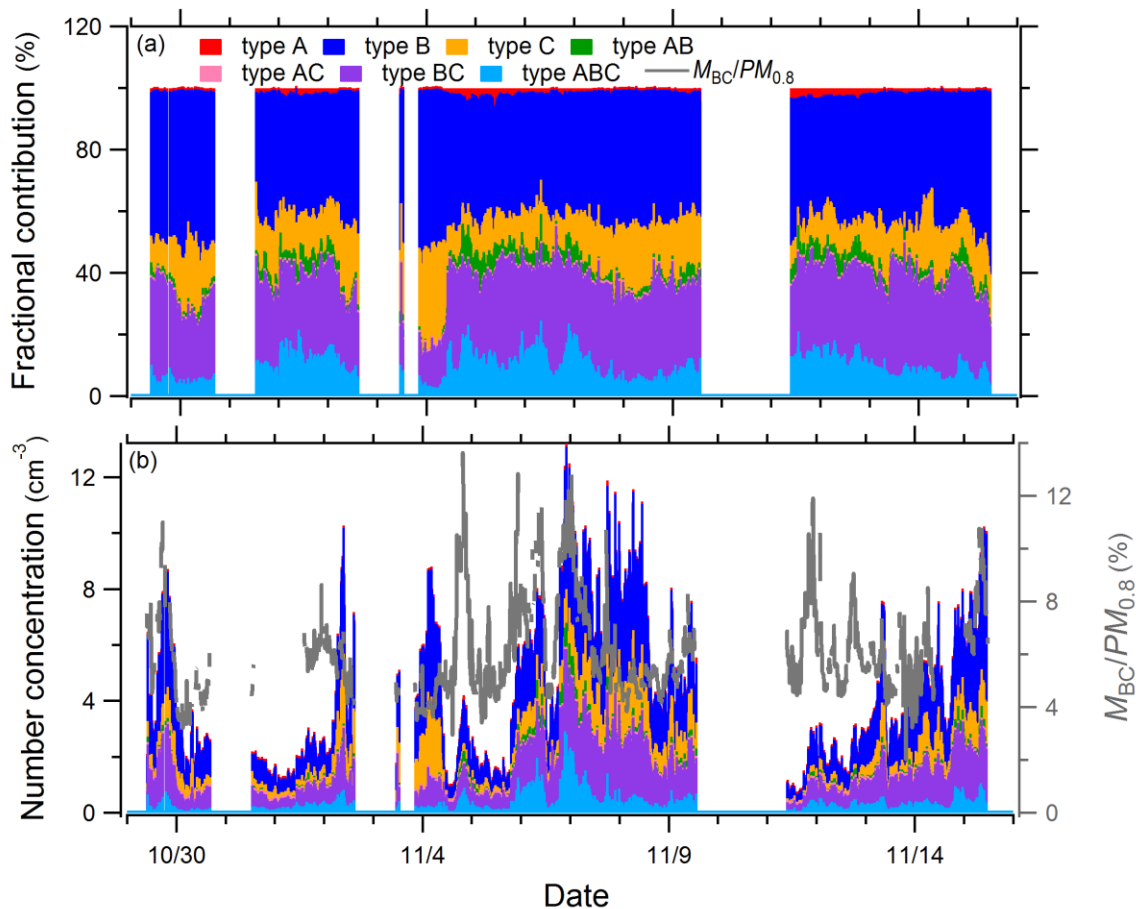


509

510

511 **Figure 3.** Spectral pattern of the classified fluorescence intensity. FL1 intensity is
 512 grouped at 100 intervals, FL2 intensity is grouped at 80 intervals and FL3 intensity is
 513 grouped at 18 intervals. Color scale is measured particle number. None fluorescent and
 514 saturating ($FL \geq 2000$ a.u.) aerosol particles were excluded. (a) FL1 intensity versus FL2
 515 intensity of total measured particles; (b) FL2 intensity versus FL3 intensity of g3 type
 516 particles; (c) FL2 intensity versus FL3 intensity of g4 type particles; (d) Numbers of g1
 517 and g2 type particles of FL3 fluorescence intensity. Because FL2 intensity of g1 and g2
 518 are below the threshold, the spectral patterns are hence not used. Dotted lines denote the
 519 threshold of each channel (200 a.u. for FL1, 80 a.u. for FL2 and 18 a.u. for FL3).

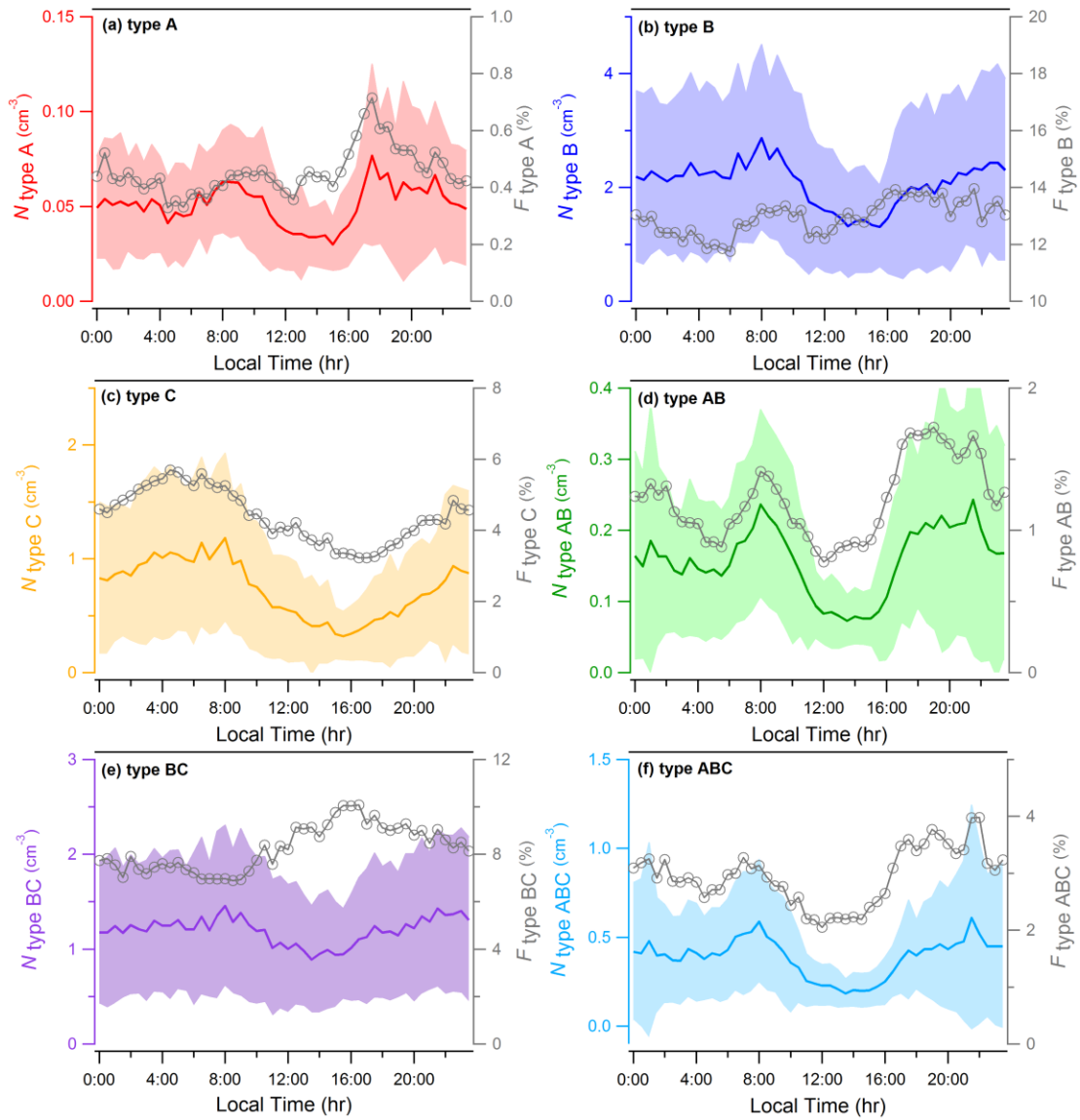
520



521

522 **Figure 4.** Time series of (a) the fractional contributions of each fluorescent type to the
 523 total FAPs and (b) number concentration (left axis) of each fluorescent type and
 524 $M_{BC}/PM_{0.8}$ (gray line, right axis). Red color indicate type A, blue color indicate type B,
 525 dark yellow indicate type C, green color indicate type AB, pink color indicate type AC,
 526 purple color indicate type BC, light blue color indicate type ABC.

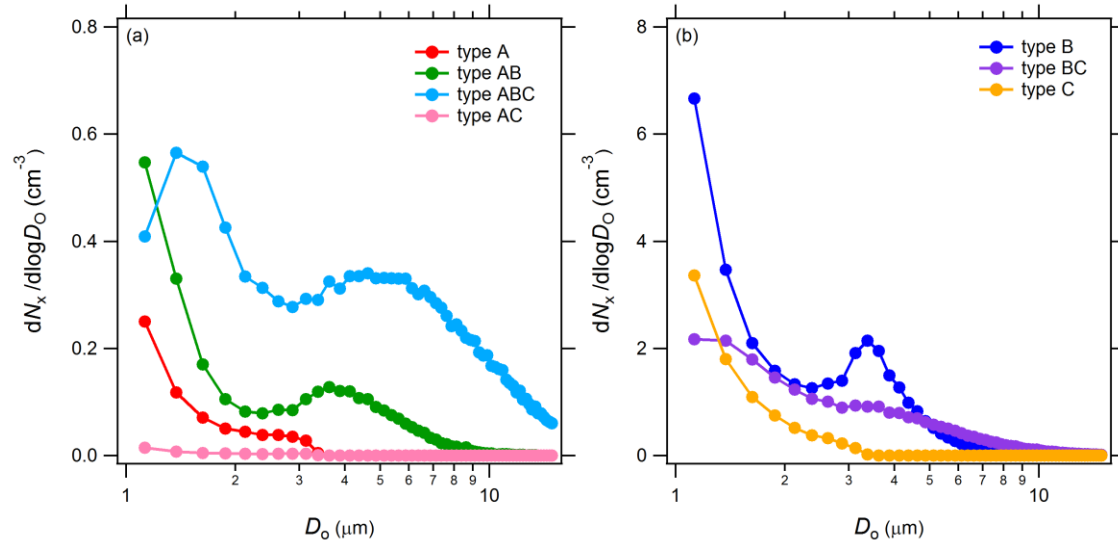
527



528

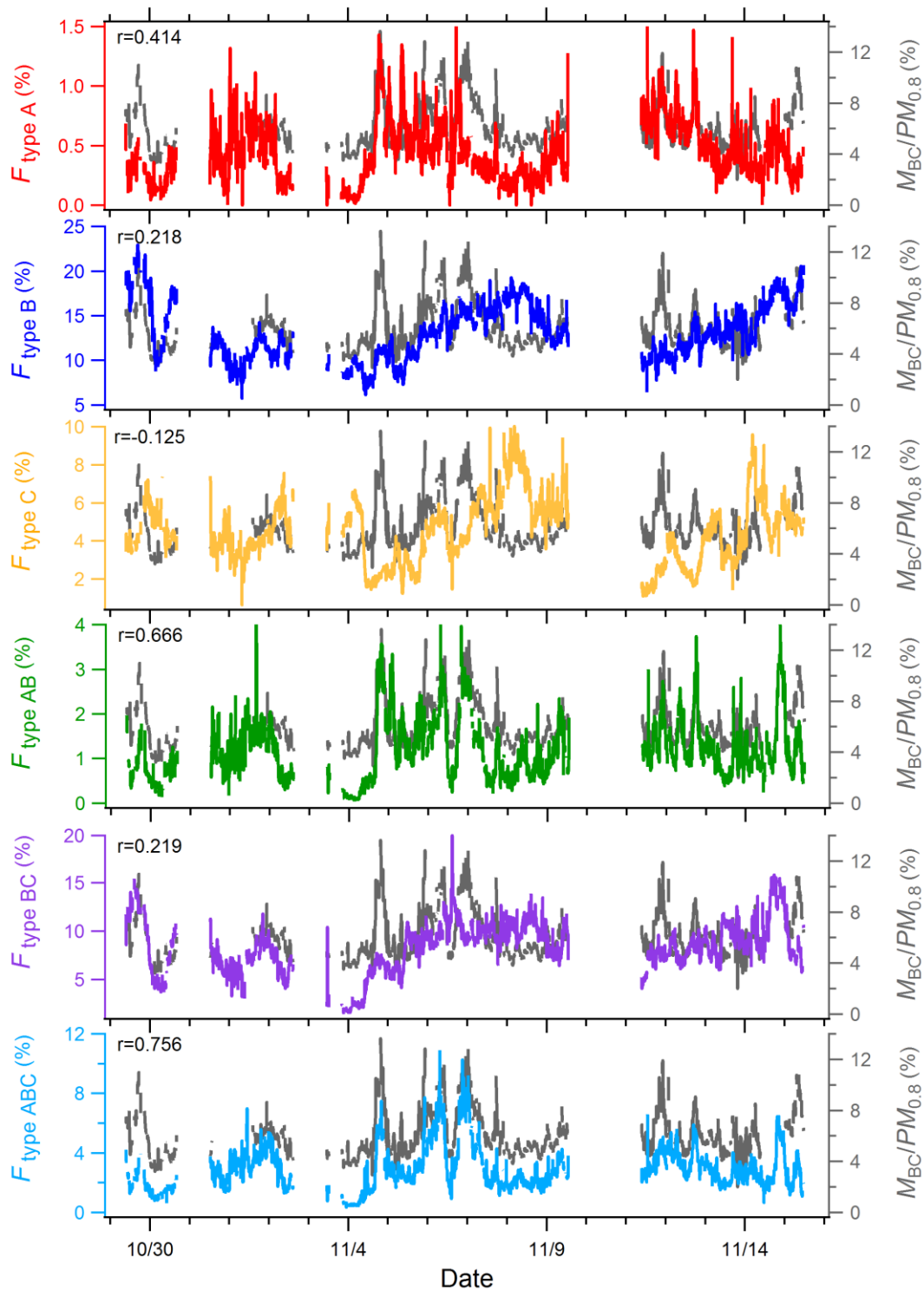
529 **Figure 5.** Diurnal variations of number concentrations of (a) type A, red, (b) type B, blue,
 530 (c) type C, dark yellow, (d) type AB, green, (e) type BC, purple and (f) type ABC, light
 531 blue. Gray line indicates the number fraction of respective fluorescent particles (right
 532 axis). Shading indicates \pm one standard deviation.

533



534

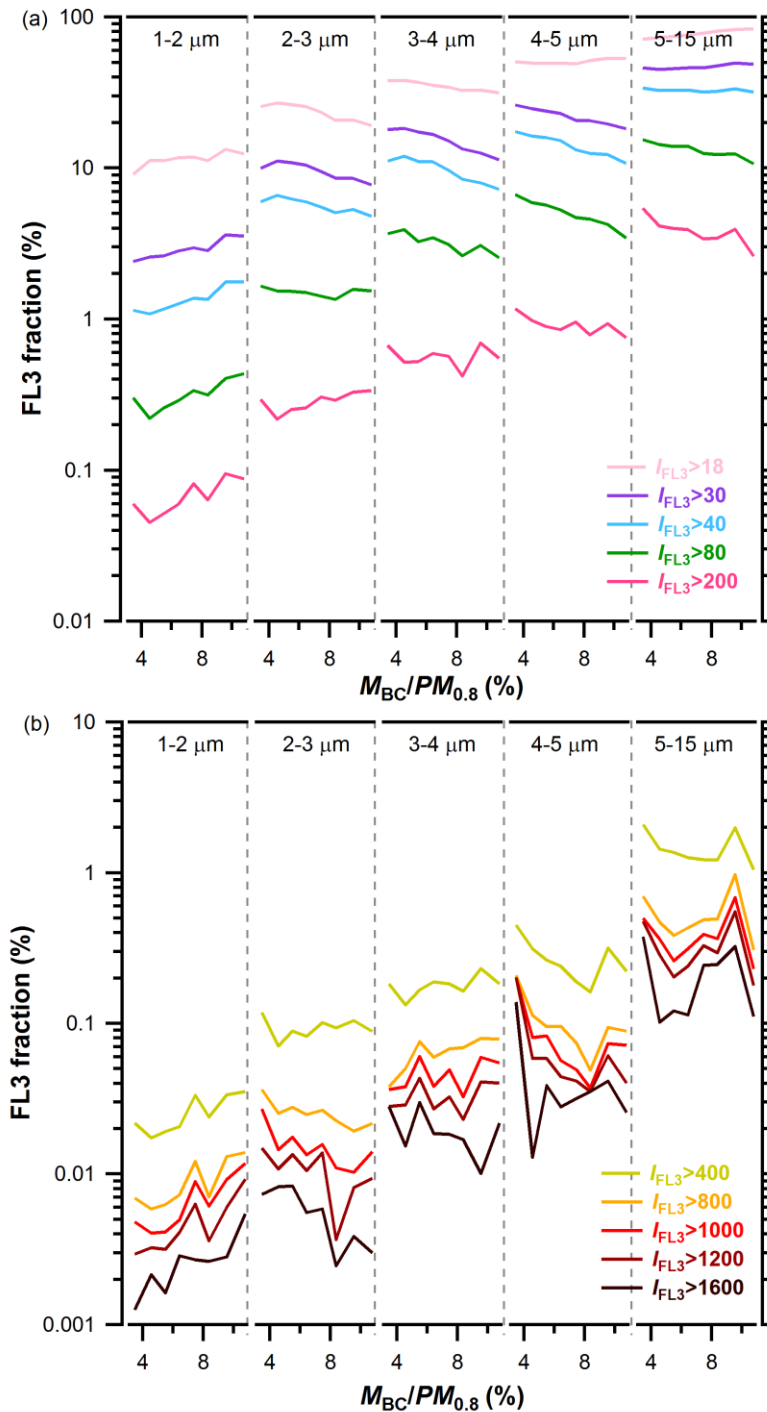
535 **Figure 6.** Mean number size distributions of (a) type A (red), type AB (green), type AC
 536 (pink) and type ABC (light blue); (b) type B (blue), type BC (purple) and type C (dark
 537 yellow).



538

539 **Figure 7.** Time series of number fractions of various fluorescent particles (left axis) and
 540 $M_{BC}/PM_{0.8}$ (gray line, right axis). r is the correlation coefficient between F_x and
 541 $M_{BC}/PM_{0.8}$.

542



543

544 **Figure 8.** Correlations of FL3 fractions with $M_{BC}/PM_{0.8}$ in different size ranges. FL3
 545 fraction is the number concentration of the subgroup ratio to the number concentration of
 546 total particles in each size bin. (a) Low fluorescent intensity group. (b) High fluorescent
 547 intensity group. The color lines represent the FL3 intensity (I_{FL3}) above the certain I_{cri} .